

Microwave stimulation of dislocations and the magnetic control of the earthquake core

A L Buchachenko

DOI: <https://doi.org/10.3367/UFNe.2018.03.038301>

Contents

1. Introduction	46
2. Magnetic catalysis of dislocation motion	47
3. Microwave reception: resonance frequencies	47
3.1 Ionic crystals; 3.2 Covalent crystals	
4. Microwave reception: nonresonance frequencies	49
5. Magnetoseismic physics of the earthquake focus	50
5.1 Magnetic perturbations and earthquakes; 5.2 Magnetic perturbations and seismotectonic deformations;	
5.3 Physical mechanics of dislocations in the focus	
6. Conclusions	52
References	52

Abstract. Microwave irradiation transforms the elasticity of solids into plasticity by controlling the dislocation mobility via magnetic interactions within the electron spin pairs on the dislocations. In ionic crystals, microwaves cause dislocations to accelerate and increase their mean free path, thus leading to a release of elastic energy; in covalent crystals, microwaves keep dislocations in place, thereby accumulating elastic energy and increasing the crystal strength. Microwave pumping at resonant Zeeman frequencies (in the magnetic resonance regime) is firm evidence of the concepts of electron spin pairs and of the magnetoplasticity phenomenon itself. However, the dominant contribution to the macroscopic transformation of elastic energy into plastic flow comes from nonresonant microwaves. These can be used to control the mechanics of diamagnetic solids, including, importantly, the earthquake focus. The observed correlation between magnetic events (such as magnetic storms and hydrodynamically generated high-power magnetic pulses) and their seismic and tectonic consequences (earthquake frequency and magnitude and deformations) indicates unambiguously that

magnetically controlling the earthquake focus provides a realistic means to prevent a catastrophe by transforming large-magnitude earthquakes into weak, low-magnitude events.

Keywords: magnetoplasticity, dislocation, magnetic effects, earthquakes, microwave dislocation stimulation, magnetic earthquake control

1. Introduction

The mechanics of diamagnetic crystals depend on the magnetic field. This phenomenon, called magnetoplasticity, seems enigmatic because crystals revealing this property have no magnetic components. It is established reliably that the source of magnetoplasticity is dislocations; the velocity of their motion depends on a magnetic field [1, 2], and this dependence is a key to the magnetically dependent mechanics. It was clear, of course, that during the motion of dislocations in a diamagnetic crystal, some paramagnetic states subjected to the magnetic-field action appear, but their nature remained enigmatic. It was proved experimentally that the source of magnetoplasticity is the dislocation + stopper system. Because any contribution of the magnetic field to the energy budget of this system is irrelevant, we should suggest that the electron spin (angular momentum) is somehow involved here and magnetic-field-controlled spin prohibitions exist in the dislocation + stopper system. However, neither a free dislocation nor a diamagnetic stopper (a Ca^{2+} type) carry a spin. Even if a stopper is paramagnetic (for example, Ni^{3+} or Cu^{2+}), the dislocation + stopper system does not become spin-selective: it does not have spin prohibitions because the spin of the initial state (a stopper-captured dislocation) and the spin of the final state (a detached one: an escaped dislocation and a remaining stopper) are the same and cannot provide magnetoplasticity.

The idea of creating a two-spin electron pair (a magnetically sensitive pair) in a stopper-captured dislocation was

A L Buchachenko Semenov Institute of Chemical Physics, Russian Academy of Sciences, ul. Kosygina 4, 119991 Russian Federation; Institute of Chemical Physics Problems, Russian Academy of Sciences, prosp. Akad. Semenov 1, 142432, Chernogolovka, Moscow region, Russian Federation; Scientific Center in Chernogolovka, Russian Academy of Sciences, ul. Lesnaya 9, 142432 Chernogolovka, Moscow region, Russian Federation; Lomonosov Moscow State University, Leninskie gory 1, 119991 Moscow, Russian Federation; Demidov Yaroslavl' State University, ul. Sovetskaya 14, 150003 Yaroslavl', Russian Federation E-mail: abuchach@chph.ras.ru, alb9397128@yandex.ru

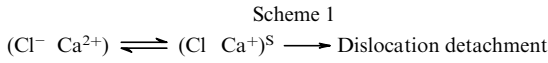
Received 19 December 2017, revised 20 February 2018

Uspekhi Fizicheskikh Nauk 189 (1) 47 – 54 (2019)

DOI: <https://doi.org/10.3367/UFNr.2018.03.038301>

Translated by M N Sapozhnikov; edited by A M Semikhatov

proposed in [3]. It is assumed that an electron is exchanged between partners, resulting in the appearance of two unpaired electrons (one at a time on the dislocation and on the stopper) and the creation of a spin pair in the singlet and triplet spin states. Thus, a dislocation captured on a calcium ion in a NaCl crystal can be represented schematically at the atomic level as $(\text{Cl}^- \text{Ca}^{2+})$, where Cl^- is the chlorine ion belonging to the dislocation (Scheme 1).



The electron transfer from Cl^- to Ca^{2+} occurs without changing the spin and creates a $(\text{Cl} \text{Ca}^+)^{\text{S}}$ two-spin pair in the singlet state S. This is important in the physics of an electron-spin pair: the captured dislocation is located in a Coulomb trap. However, the Coulomb interaction in a new $(\text{Cl} \text{Ca}^+)^{\text{S}}$ pair is absent and the stopper does not retain the dislocation, which detaches and continues its motion.

2. Magnetic catalysis of dislocation motion

The arrangement of electron spins in singlet and triplet states is presented in Fig. 1 and their energy levels are shown in Fig. 2.

The triplet state in a magnetic field is split into three substates T_0 , T_+ , and T_- with the electron spin projections 0, +1, and -1 (Fig. 1). The magnetic field (Zeeman interaction) induces only $S-T_0$ transitions, and therefore only the S and T_0 states are populated in the absence of a microwave field. A resonance microwave field changes the orientation of electron spins, inducing the transition of a pair from the T_0 state to the T_+ and T_- states (Fig. 2) and partially depleting the T_0 level, which is now additionally populated during $S-T_0$ transitions due to spin dephasing (Fig. 3).

This means that the microwave field additionally increases the triplet state lifetime of the pair, thereby increasing the dislocation detachment probability. In other words, the pair is a microwave receiver whose pumping at Zeeman frequencies $g\beta H$ drastically increases the lifetime of the triplet pair with the Coulomb interaction switched off. As

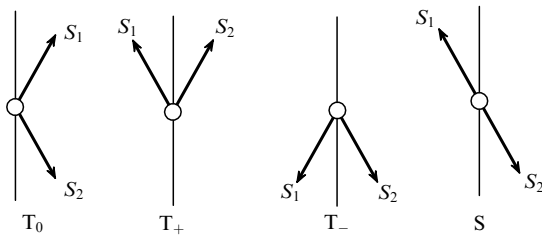


Figure 1. Arrangement of electron spins S_1 and S_2 in singlet and triplet spin states.

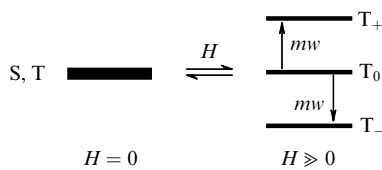


Figure 2. Energy level diagrams of a spin pair in the zero ($H = 0$) and strong ($H \gg 0$) magnetic fields. The microwave field mw induces transitions from the T_0 state to the T_+ and T_- states.

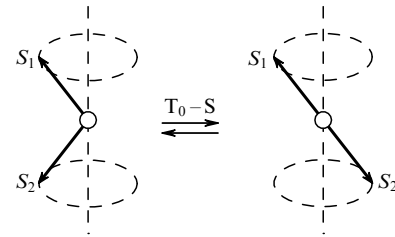
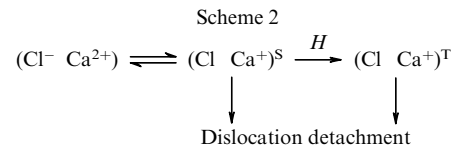


Figure 3. Transformation (spin conversion) of the T_0 and S states.

a result, the mean free path of dislocations should increase at these frequencies. Magnetic fields, both permanent and microwave, excite the pair to the triplet state, from which the dislocation cannot return to the initial trapped state. Thus, the magnetic field accelerates and catalyzes the motion of dislocations, and this magnetic catalysis creates magneto-plasticity as a physical phenomenon. Scheme 2 illustrates this process at the atomic level [4, 5].



3. Microwave reception: resonance frequencies

Magnetic resonances at Zeeman frequencies $g\beta H$ in a spin pair are the best proof of the atomic-molecular concepts of magneto-plasticity. Resonances are detected in both ionic and covalent crystals (diamond, silicon, germanium), which means that the trapped dislocation with an electron-spin pair created on it operates as a microwave receiver.

3.1 Ionic crystals

The drastic acceleration of dislocations at Zeeman resonances was discovered in 1998 (Fig. 4) in Ca^{2+} -doped NaCl crystals [6]. The microwave effect was considerable, and the mean free path of dislocations increased by 50 to 70% in these resonance fields. The three resonance frequencies $g\beta H$ correspond to the three types of spin pairs and seem to include partially spin-forbidden resonances, although this

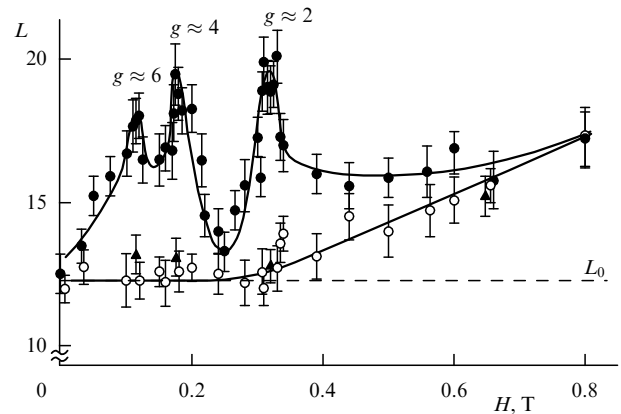


Figure 4. Increase in the dislocation mean free path in resonance fields at frequencies $g_1\beta H$ ($g \approx 6$), $g_2\beta H$ ($g \approx 4$), and $g_3\beta H$ ($g \approx 2$). Open circles show the dislocation mean free path in the absence of a microwave field (lower curve). L_0 is the start path in the absence of a field.

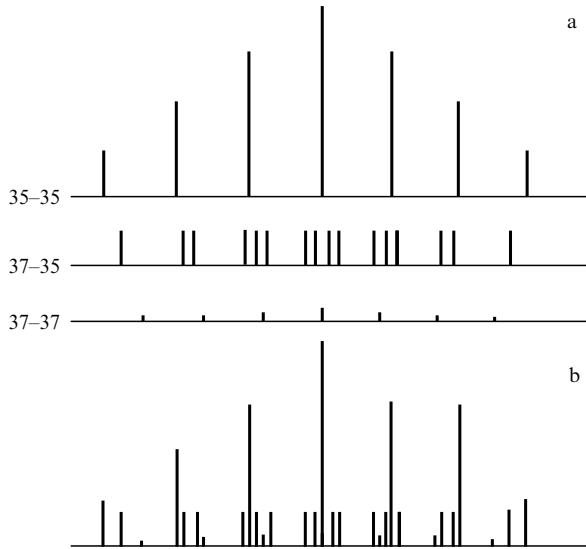


Figure 5. EPR spectrum of the Cl_2^- radical as a superposition of its 16 magneto-isotopic resonances: (a) three isotopic pairs, (b) complete spectrum.

interpretation is ambiguous. It is only clear that this is, in fact, the electron paramagnetic resonance (EPR) observed by the motion of dislocations. As regards EPR, the resonance intensity is maximal when a permanent and an alternating field are orthogonal and decreases by an order of magnitude in parallel fields [7].

The electron transfer (Scheme 1) and the creation of a $(\text{Ca}^+ \text{Cl})$ spin pair are the first steps to magnetoplasticity. The chlorine atom Cl in the NaCl lattice attaches to the Cl^- anion [8], forming a new $(\text{Ca}^+ \text{Cl}_2^-)$ spin pair. This pair is a microwave receiver providing magnetoplasticity. The ^{35}Cl (76%) and ^{37}Cl (24%) isotopes have close magnetic moments ($0.82\mu_B$ and $0.68\mu_B$) and the same spin $3/2$. The Cl_2^- radical has 16 electron–nucleus resonances $((2I_{35} + 1)(2I_{37} + 1) = 16)$ and is represented in the crystal by the superposition of $(^{35}\text{Cl}^{35}\text{Cl})^-$, $(^{35}\text{Cl}^{37}\text{Cl})^-$, and $(^{37}\text{Cl}^{37}\text{Cl})^-$ in the relative fractions $9/16$, $6/16$, and $1/16$ [8].

The electron–nucleus microwave spectrum (EPR spectrum) schematically presented in Fig. 5 exactly corresponds to the experimental EPR spectrum [8, 9], and the distances between EPR lines determine isotropic hyperfine interaction (HFI) constants. However, both the g factor and hyperfine interaction B in the Cl_2^- radical are strongly anisotropic and axially symmetric. The components of the g factor are $g_{xx} = g_{yy} \approx 2.044$ and $g_{zz} = 2.001$. The HFI components are also known: $B_{xx} = B_{yy} = -25.8 \text{ G}$, $B_{zz} = +51.7 \text{ G}$ [9].

The Cl_2^- radical occurs in different positions in a NaCl crystal, and hence its molecular axes have different orientations with respect to the crystallographic axes. Because of the anisotropy of tensors G and B , the Cl_2^- radical reveals numerous electron–nucleus resonances. Some of them are weak and are not observed in the spectra of dislocation path lengths, but many have almost coinciding frequencies, and their superposition makes the total contribution to the acceleration of dislocations. Such numerous resonances were experimentally observed in many fundamental studies by Alshits and coworkers (see review [1] of these papers).

Numerous resonances were also observed in the Earth field; they fall into the radiofrequency range $\sim 1 \text{ MHz}$ and are accompanied by the acceleration of dislocations and a

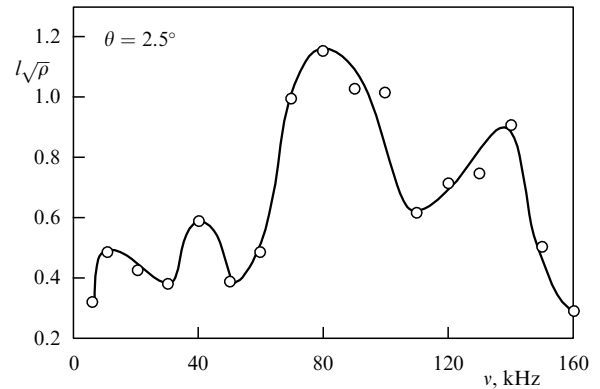


Figure 6. Normalized magnetoresonance spectrum of dislocation motion in NaCl [13].

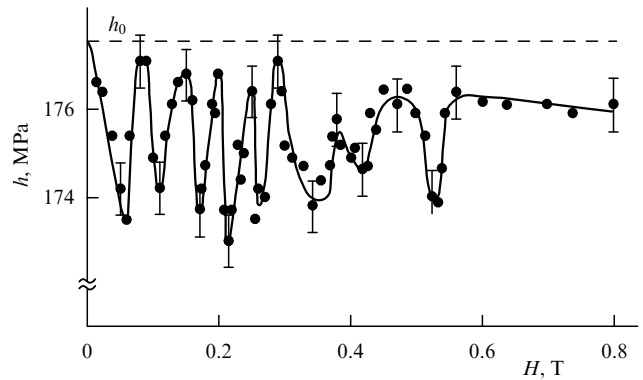


Figure 7. Microhardness of an $\text{NaCl}(\text{Eu}^{2+})$ crystal as a function of a permanent magnetic field under microwave pumping. Eight resonance holes in the microhardness are distinctly observed; h_0 is the microhardness in the zero field (dashed straight line).

decrease in the microhardness of ZnO, LiF, potassium triglycine sulfate, and hydrogen phthalate crystals [10, 11]. An example of numerous resonances is shown in Fig. 6. For the angle $\theta = 2.5^\circ$ between the edge a of a NaCl single crystal and Earth's magnetic field direction, only four distinct resonances are detected. Here, the linear path length l of dislocations is normalized to the dimensionless path $l\sqrt{\rho}$ (where ρ is the dislocation density), i.e., to the ratio of the path length to the mean distance between dislocations. A considerably greater number of resonances is often observed [12, 13]. The lifetime of a two-spin pair estimated from the low-frequency resonance was $\tau \approx 5 \times 10^{-7} \text{ s}$ [1].

Resonantly induced large-scale displacements of dislocations in NaCl are observed in the pulsed microwave pumping regime [13]: in the case of a pulsed resonance for $0.5 \mu\text{s}$ and the pump amplitude 0.176 G , dislocations are displaced over a distance of about $10^2 \mu\text{m}$. In the same crystal in the stationary pumping regime with the amplitude of 0.025 G , the displacement of dislocations over this distance requires about 5 min. It is clear that the pulse produces an explosive, almost coherent, avalanche of running dislocations. Such a regime actually ensures the depletion of dislocations in the crystal. We note that the pulsed microwave irradiation of an earthquake focus also produces strong effects (see Section 5).

A strong effect was also discovered in Eu^{2+} -doped NaCl crystals [14]. Here, seven resonances were observed at which

the microhardness of crystals drastically decreased (Fig. 7). They can appear because the nuclear spin 5/2 of europium causes the hyperfine splitting of Zeeman levels, thereby increasing the number of electron–nucleus resonances. The microwave pumping governs the spin evolution of pairs, in this way controlling the motion of dislocations and microhardness.

3.2 Covalent crystals

A dislocation in covalent crystals is a chain of atoms with partially broken chemical bonds, i.e., with free valences and unpaired electrons on some atoms of the chain (see details in [4]). As dislocations meet, a spin pair can be produced in one of the four spin states, S, T₀, T₊, and T₋, each with a statistical weight of 1/4. In the singlet state S, valences recombine and dislocations stop, coupled by a chemical bond. Recombination in the triplet T₊ and T₋ states is completely spin-forbidden (if the hyperfine interaction is absent), while recombination into the T₀ state requires spin conversion from T₀ to S (see Fig. 3). A microwave resonance field induces transitions from the T₊ and T₋ states to the T₀ state (see Fig. 2), from which a transition to the S state occurs, where the recombination of dislocations take place. Thus, spin conversion in a pair occurs in the direction opposite to that in ionic crystals. The microwave field stimulates the linking and immobilization of dislocations, i.e., induces the dislocation strengthening of covalent-atomic crystals.

Such a strengthening in silicon was observed in [15, 16]. The decrease in the path length of dislocations induced by the microwave field reached 30–40% and had a resonance character (Fig. 8).

A strong coupling of dislocations in silicon by microwave radiation is reliably supported by a considerable increase in the voltage required for displacing a fixed dislocation [17]. Figure 9 clearly demonstrates that a dislocation is fixed at the EPR frequency and releasing it requires a considerable additional shear voltage.

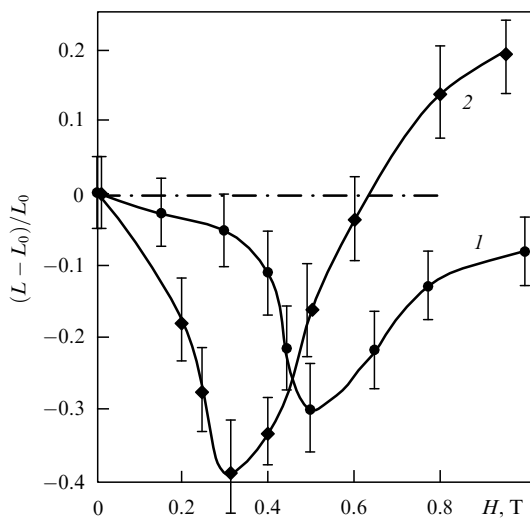


Figure 8. Dislocation path length L in a silicon single crystal as a function of the magnetic field upon microwave pumping. The magnetic field effect exhibits the Zeeman interaction anisotropy: curve 1 corresponds to the microwave field directed along the [100] plane, curve 2 to the field directed along the [011] plane, L_0 is the dislocation path length in the absence of the magnetic field.

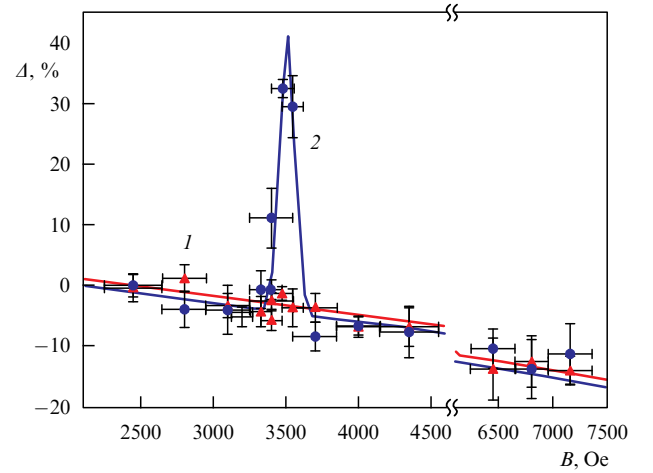


Figure 9. (Color online.) Change in the displacement stress Δ as a function of the magnetic field B . Curve 1 shows Δ in the absence of microwave irradiation, curve 2 in its presence. The resonance increase in Δ corresponds to the EPR frequency fixing a dislocation [16].

4. Microwave reception: nonresonance frequencies

Numerous resonances reliably prove the existence of two-spin pairs and the concept of magnetoplasticity. However, resonance effects are only a method for studying and understanding the physics of dislocations. It is unlikely that even numerous resonances can provide a considerable displacement of dislocations and the macroscopic conversion of the elastic energy into a plastic flow. For this purpose, non-resonance fields are much more efficient.

The precession frequency of the electron spin of the first partner of a spin pair is

$$\omega_1 = g_1\beta H + \sum a_i m_i, \quad (1)$$

where the first term in the right-hand side is the contribution of the Zeeman interaction to precession, the second term is the contribution of the hyperfine interaction, a_i are hyperfine coupling constants, m_i are projections of magnetic nuclear spins of the first partner, and the sum is taken over all i nuclei. The precession frequency of the electron spin of the second partner with nuclei j is similarly given by

$$\omega_2 = g_2\beta H + \sum a_j m_j. \quad (2)$$

Spin conversion occurs due to precession of electrons in the pair; the difference between precession frequencies $\Delta\omega = \omega_1 - \omega_2$ produces a dephasing of spins, i.e., spin conversion:

$$\Delta\omega = [(g_1 - g_2)\beta H] + \left(\sum a_i m_i - \sum a_j m_j \right). \quad (3)$$

The spin change time in the electron-spin pair, i.e., the spin conversion time τ_S , is the total dephasing time (rotation of spins in the pair by π) given by

$$\tau_S = \left\{ [(g_1 - g_2)\beta H] + \left(\sum a_i m_i - \sum a_j m_j \right) \right\}^{-1}. \quad (4)$$

The complete and illustrative picture of spin conversion is shown in Fig. 10. The T₀–S spin conversion is produced by both the Zeeman and hyperfine interaction, but the T₊–S and T₋–S transitions are stimulated only by the hyperfine

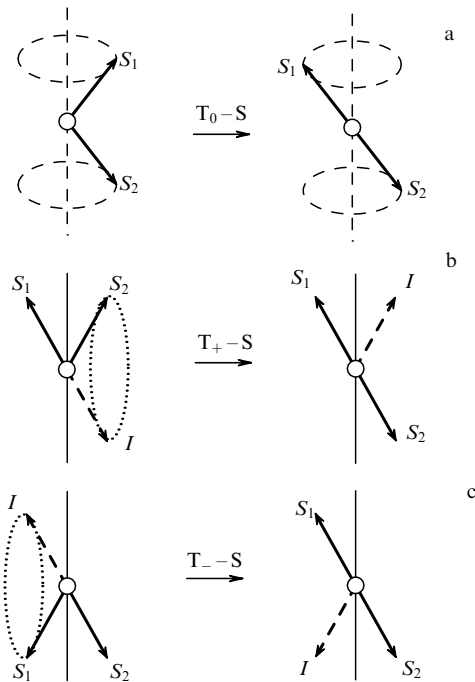


Figure 10. Vector representations of the (a) T_0-S , (b) T_+-S , and (c) T_--S conversion; S_1 and S_2 are the electron spins of the partners, I is the nuclear spin.

interaction; in this case, an electron and a nucleus exchange their angular momenta, performing the common precession shown by the dots in Figs 10b, c.

The influence of a microwave oscillating magnetic field on the electron spins of the pair depends on the frequency ω of this field, i.e., on the oscillation period $\tau_0 = \omega^{-1}$. Low-frequency fields (for which $\tau_0 > \tau_S$) cause only spin dephasing; they act as permanent fields, because the field oscillation period is much longer than the $S-T$ spin conversion time. In other words, the electron-spin pair ‘sees’ any low-frequency field oscillating at a frequency $\tau_0^{-1} < \tau_S^{-1}$ as a permanent field performing the $S-T$ conversion via dephasing.

At resonance frequencies, when the field oscillation frequency coincides with the Zeeman frequency, the $S-T$ conversion occurs due to the spin flip. The density of such resonance fields is low, even in the case of numerous resonances (discussed in Section 3). Therefore, the influence of resonance fields can certainly be ignored (except exotic cases when frequencies are especially tuned to resonance). This means, in fact, that all the magnetic fields oscillating at frequencies lower than ≈ 100 MHz can be considered permanent with respect to a short-lived receiver—an electron-spin pair. Magnetic fields oscillating at frequencies above 100 MHz (if they are nonresonant) are inefficient because the slow spin system weakly responds to high-frequency oscillations.

5. Magnetoseismic physics of the earthquake focus

We now consider an intriguing question: Is it possible to apply the physics of magnetoplasticity, both in permanent and in alternating fields, to the physics of earthquakes? In other words, is it possible to use the magnetic control of dislocations as means of faulting elastic stresses in the

earthquake focus to avoid a catastrophe by transforming a large-magnitude earthquake to a weak, small-magnitude one? The answer to this question should be sought in correlations between magnetic and seismic phenomena, in their coincidences or noncoincidences; no other way is feasible. In the case of coincidences, the question formulated above makes sense, whereas noncoincidences make this question irrelevant.

The search for correlations can be performed in two different ways, which lends credibility to it. We first consider the relation between earthquakes and magnetic perturbations, natural (magnetic storms) and artificial (electromagnetic irradiation of the earthquake focus by discharges from a magnetohydrodynamic generator). Second, we analyze the influence of electromagnetic fields on the magnitude and velocity of seismotectonic deformations.

We note at once that magnetic control operates on the atomic-molecular level (creation and motion of dislocations). It stimulates the elastic energy drop preceding the destruction. Its purpose is to exclude or avoid destruction. The formation of microcracks and their association and macroscopic destruction are processes not subjected to magnetic influence.

We note that two types of magnetic phenomena are known in seismic processes: one of them precedes earthquakes by stimulating or suppressing them, while the other accompanies earthquakes as their consequence. The first phenomenon can be reasonably called magneto-seismic (it is considered in this article), while the other can be called seismo-magnetic. This last occurs as a reflection or consequence of destructive processes: the formation of cracks and the generation of electromagnetic radiation during an electric discharge between their banks.

5.1 Magnetic perturbations and earthquakes

The two events, magnetic perturbations and earthquakes, were excellently analyzed in [17]. Magnetic storms (1973–2010) were treated as perturbations, with the storm onset taken as the zero time. The number of large-magnitude earthquakes ($M \geq 5$) that took place 60 min before the sudden storm onset and 60 min after it was then determined. If these events are independent, 405 analyzed earthquakes must be distributed almost equally. However, this expectation is not confirmed: 230 earthquakes occurred before the storm and only 173 after it. This shows that the frequency of strong earthquakes ($M \geq 5$) decreases after the storm by more than 30%, i.e., the foci partially lose their elastic energy. This 30% decrease means that a magnetic storm eliminates each third large-magnitude earthquake, transforming it into a small-magnitude one. The thick horizontal straight line in Fig. 11 is drawn for earthquakes with $M = 6.6$. We can see that 8 earthquakes with $M > 6.6$ occurred before the storm and only 2 after it. Figure 12 shows how the frequency of large earthquakes decreases after the storm, and the frequency distribution shifts to the lower frequencies. The authors of [17] make the statistically reliable conclusion that magnetic perturbation in the form of storms suppresses powerful earthquakes. We see below that the key word here is powerful. Effects of magnetic storms were also discussed in [18].

Extensive experiments performed for many years have shown that artificial magnetic perturbations from an MHD generator also corroborate the relation between magnetic and seismic phenomena [19–21]. For example, analysis of the number of earthquakes 30 days before an MHD pulse (m)

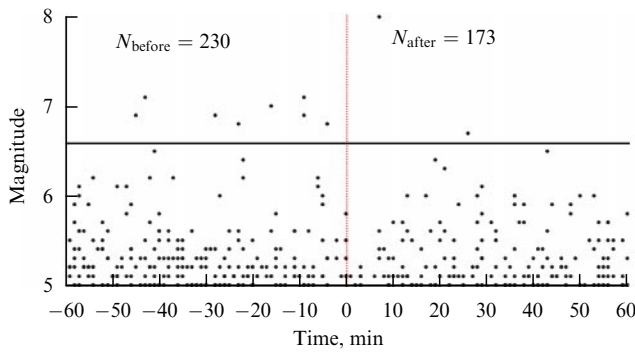


Figure 11. Earthquakes with magnitudes $M \geq 5$ at time intervals of ± 60 min with respect to the storm onset time ($t = 0$).

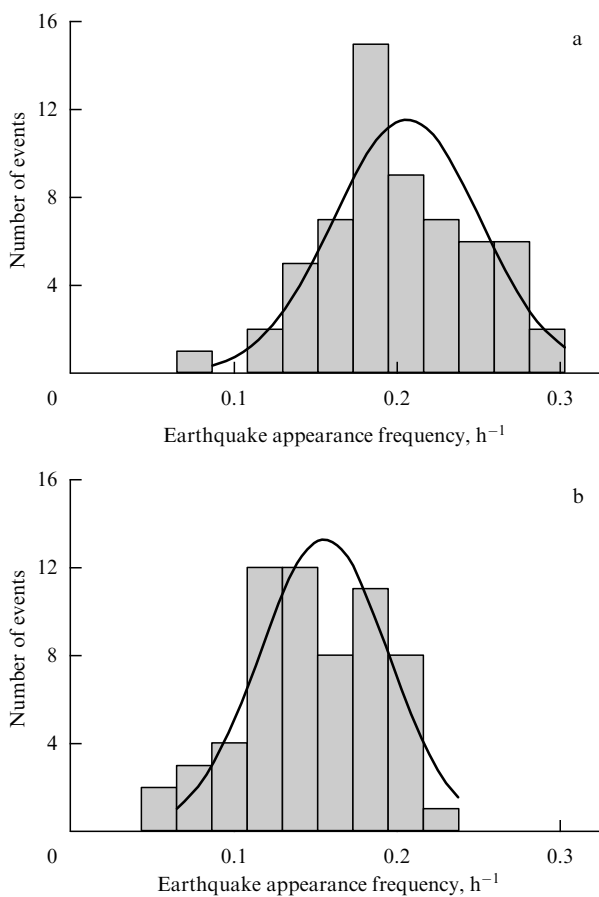


Figure 12. Earthquake distributions with respect to the appearance frequency in hour intervals (a) before a magnetic storm and (b) after it. Smooth curves are normal distributions approximating the earthquakes observed.

and 30 days after the pulse (n) showed that $m/n > 1$ (about 1.15–1.45) for large-magnitude earthquakes, but $m/n < 1$ (about 0.8–0.9) for weak earthquakes [19].

The total result of numerous observations of magneto-seismic correlations (irrespective of magnetic perturbations, natural or artificial) is unambiguous: magnetic perturbations suppress large-magnitude earthquakes but stimulate or induce weak, low-magnitude earthquakes. The frequency of the former decreases, while the frequency of the latter increases. There is another enigmatic property, namely, the

5–6 day delay of a seismic response to the electromagnetic signal [20].

At first glance, these effects seem intriguing and contradictory. They are commonly considered to be two independent phenomena, and this standpoint makes them inexplicable. But this is a single phenomenon rather than two phenomena: the suppression of a large-magnitude seismic event means its transformation into a weak, small-amplitude earthquake. The increase in the number of weak earthquakes is a direct consequence of the decrease in the number of powerful earthquakes. Such a synchronism in the suppression of strong earthquakes and stimulation of weak earthquakes suggests that magnetic perturbations stimulate a partial drop in the elastic energy trapped in the earthquake focus by decreasing its amount and decreasing the magnitude of dangerous earthquakes. Of course, it is impossible to eliminate an earthquake, but it is possible to transform it into a weak and less damaging one.

5.2 Magnetic perturbations and seismotectonic deformations

The stimulation of weak earthquakes by eliminating stressed foci should inevitably be revealed in seismotectonic deformations. This prediction was indeed reliably confirmed in [21–24] by direct measurements of deformations upon irradiation of earthquake foci by pulses from an MHD generator. Both in the Garm region, Tajikistan (1975–1978, 34 MHD generator firings) and in the North Tien Shan near Bishkek (1983–1990, 113 firings), the mean deformation rates increased by 10–20 times. Figures 13 and 14 clearly demonstrate this effect: both deformations $\varepsilon(t)$ and their velocities $v(t)$ drastically increase during irradiation with electromagnetic fields from MHD generators. These observations actually demonstrate a

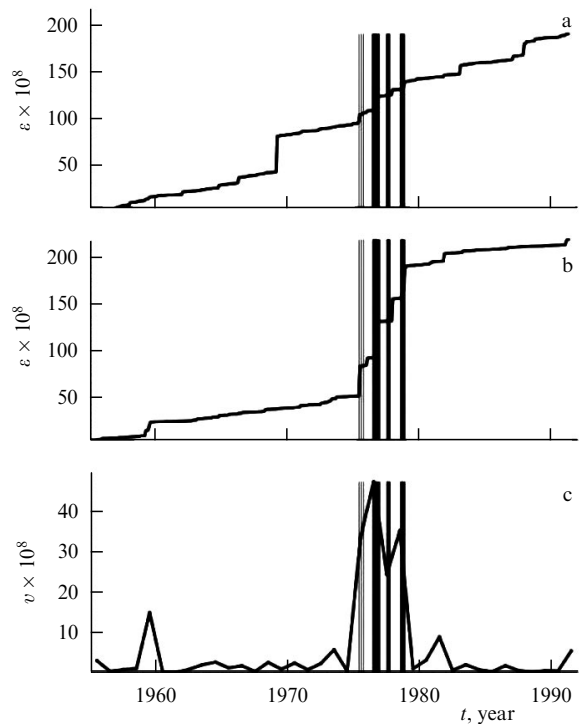


Figure 13. Tectonic deformations ε in (a) the Garm region and (b) its upper layer before and after irradiation by electromagnetic pulses from MHD generators (pulses are shown by vertical straight lines). The deformation velocity shown in the figure is maximal at the pulse instants.

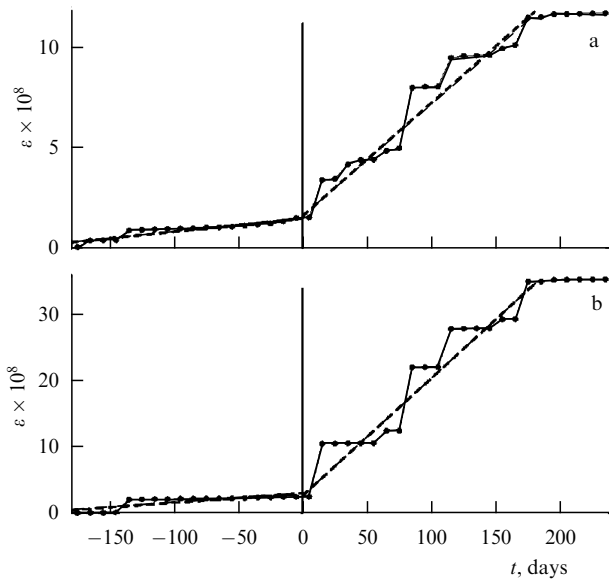


Figure 14. Tectonic deformations ε in (a) the Garm region and (b) its upper layer before irradiation by electromagnetic pulses from MHD generators ($t < 0$) and after it ($t > 0$). The instant of pulses corresponds to $t = 0$.

slow plastic deformation of the focus stimulated by magnetic pulses.

Thus, in Garm, the deformation rate before a pulse was 2.42 (in generally accepted conventional units), while in the pulsed regime the deformation rate was almost 20 times higher (38.8) [23]. It was also found that the deformation rate after the pulses was lower than before them. This effect can be reasonably explained by the fact that a significant decrease in the elastic energy stimulated by pulses depletes the focus of the excessive elastic energy.

5.3 Physical mechanics of dislocations in the focus

The magnetically stimulated release of the elastic energy of the focus occurs through dislocations. This statement would be undeniable if the focus were a single crystal [25]. However, it is nonuniform, in both its chemical composition and its structural morphology. Numerous inhomogeneities produce numerous surfaces—interfaces between microcrystals and between regions with different densities, compressibilities, and shear moduli. Slipping along these planes could be the universal mechanism of elastic energy release, and no earthquakes would have occurred in the framework of this mechanism. It is clear that this macroscopic mechanism operates weakly, probably due to strong friction between slip surfaces in a strongly compressed focus. This suggests that the elastic energy can be accumulated on the atomic-molecular level and is released in a plastic flow of dislocations.

A key question in understanding magnetoseismic effects is then the mechanics of dislocations on interfaces. A dislocation on an interface (for example, of NaCl and CaO crystals) can produce two effects: relay transfer and local microslipping. A dislocation that escapes, for example, from NaCl to the interface cannot overcome the interface because of the incompatibility of the atomic structures of the contacting crystals and the difference in their atomic potentials. However, it is for the same reason that a dislocation from NaCl can initiate a dislocation in CaO, and this phenomenon can be treated as a relay of dislocations. Another effect is also possible. A change in potentials can initiate a microscopic

shear, microslipping along the interface, which can add to produce local microdisplacements along the slip surface. It is possible that a delay between the electromagnetic pulse and seismic response is caused by this microslipping (see above).

Any tangential stresses in interfaces inevitably produce shear deformations and create new dislocations, providing their relay. We can assume that the focus is saturated with trapped ‘sleeping’ dislocations, and a microwave magnetic field induces their ‘awakening’, stimulating their motion and decreasing the amount of elastic energy stored. In the framework of these concepts, all the magnetoseismic effects considered above acquire a physically reasonable explanation.

6. Conclusions

The magnetoplasticity of crystals induced by microwave fields is a remarkable phenomenon, opening the way for magnetic control of the mechanics of solids. The mechanics of the earthquake focus is especially important. A high correlation in a series of magnetoseismic events shows that the microwave magnetic control of the earthquake focus can be performed artificially, providing a partial release of the elastic energy of the focus and transforming a dangerous, high-magnitude earthquake into a weakened, small-magnitude one.

Acknowledgements

The author thanks V I Alshits, V V Kveder, N T Tarasov, and A V Gul’elmi for critical comments and stimulating discussions and the Russian Scientific Foundation for support (grant no. 14-23-00018). Critical comments by three referees are appreciated and have been taken into account.

References

1. Alshits V I et al. *Phys. Usp.* **60** 305 (2017); *Usp. Fiz. Nauk* **187** 327 (2017)
2. Morgunov R B *Phys. Usp.* **47** 131 (2004); *Usp. Fiz. Nauk* **174** 1231 (2004)
3. Buchachenko A L *JETP* **102** 795 (2006); *Zh. Eksp. Teor. Fiz.* **129** 909 (2006)
4. Buchachenko A L *JETP* **105** 593 (2007); *Zh. Eksp. Teor. Fiz.* **132** 673 (2007)
5. Buchachenko A L *JETP* **105** 722 (2007); *Zh. Eksp. Teor. Fiz.* **132** 827 (2007)
6. Golovin Yu I et al. *JETP Lett.* **68** 426 (1998); *Pis'ma Zh. Eksp. Teor. Fiz.* **68** 400 (1998)
7. Golovin Yu I, Morgunov R B Shmurak S Z *Phys. Dokl.* **43** 340 (1998); *Dokl. Ross. Akad. Nauk* **361** 352 (1998)
8. Castner T G, Känzig W J. *Phys. Chem. Solids* **3** 178 (1957)
9. Atkins P W, Symons M C R *The Structure of Inorganic Radicals. An Application of Electron Spin Resonance to the Study of Molecular Structure* (Amsterdam: Elsevier, 1967); Translated into Russian: *Spektry EPR i Stroenie Neorganicheskikh Radikalov* (EPR Spectra and the Structure of Inorganic Radicals) (Moscow: Mir, 1970)
10. Alshits V I et al. *Phys. Solid State* **55** 2289 (2013); *Fiz. Tverd. Tela* **55** 2176 (2013)
11. Alshits V I et al. *Phys. Solid State* **54** 324 (2012); *Fiz. Tverd. Tela* **54** 305 (2013)
12. Alshits V I et al. *JETP Lett.* **98** 28 (2013); *Pis'ma Zh. Eksp. Teor. Fiz.* **98** 33 (2013)
13. Alshits V I et al. *JETP Lett.* **104** 353 (2016); *Pis'ma Zh. Eksp. Teor. Fiz.* **104** 362 (2016)
14. Golovin Yu, Morgunov R, Baskakov A *Mol. Phys.* **100** 1291 (2002)
15. Osip'yan Yu A et al. *JETP Lett.* **79** 126 (2004); *Pis'ma Zh. Eksp. Teor. Fiz.* **79** 158 (2004)

16. Badylevich M V et al. *Phys. Status Solidi C* **2** 1869 (2005)
17. Gul'elmi A V, Lavrov I P, Sobisevich A L *Soln.-Zem. Fiz.* **1** 98 (2015)
18. Zakrzhevskaya N A, Sobolev G A *Fiz. Zemli* (4) 3 (2002)
19. Savin M G, Smagin S I *Vestn. Dal'nevostoch. Otd. Ross. Akad. Nauk* (2) 129 (2009)
20. Tarasov N T *Dokl. Ross. Akad. Nauk* **353** 542 (1997)
21. Tarasov N T, Tarasova N V *Izv. Phys. Solid Earth* **47** 937 (2011); *Fiz. Zemli* (10) 82 (2011)
22. Tarasov N T *Dokl. Earth Sci.* **433** 1088 (2010); *Dokl. Ross. Akad. Nauk* **433** 689 (2010)
23. Tarasov N T et al. *Vulkanolog. Seismolog.* (5) 152 (1999)
24. Tarasov N T, Tarasova N V *Ann. Geophys.* **47** 199 (2004)
25. Buchachenko A L *Phys. Usp.* **57** 92 (2014); *Usp. Fiz. Nauk* **184** 101 (2014)